EURASIP Journal on Applied Signal Processing 2005:6, 844–851

System Performance of Concatenated STBC and Block Turbo Codes in Dispersive Fading Channels

Yinggang Du
Department of Electronic Engineering, The Chinese University of Hong Kong, Shatin, NT, Hong Kong
Email: ygdu@ee.cuhk.edu.hk
Department of Electronic Engineering, Nanjing University of Science & Technology, Nanjing, Jiangsu 210094, China

Kam Tai Chan
Department of Electronic Engineering, The Chinese University of Hong Kong, Shatin, NT, Hong Kong
Email: ktchan@ee.cuhk.edu.hk

Received 30 September 2003; Revised 15 July 2004

A new scheme of concatenating the block turbo code (BTC) with the space-time block code (STBC) for an OFDM system in dispersive fading channels is investigated in this paper. The good error correcting capability of BTC and the large diversity gain characteristics of STBC can be achieved simultaneously. The resulting receiver outperforms the iterative convolutional Turbo receiver with maximum a posteriori probability expectation-maximization (MAP-EM) algorithm. Because of its ability to perform the encoding and decoding processes in parallel, the proposed system is easy to implement in real time.

Keywords and phrases: block turbo code, space-time block code, concatenation, OFDM, convolutional turbo code.

1. INTRODUCTION

In wireless communications, frequency-selective fading in unknown dispersive channels is a dominant problem in high data rate transmission. The resulting multipath effects reduce the received power and cause intersymbol interference (ISI). Orthogonal frequency division multiplexing (OFDM) is often applied to combat this problem [1]. OFDM is a special case of multicarrier transmission, where a single data stream is distributed and transmitted over a number of lower transmission rate subcarriers. Therefore, OFDM in effect slices a broadband frequency-selective fading channel into a set of parallel narrow band flat-fading channels.

In a flat-fading channel, the extra transmit diversity gain can be obtained by applying space-time block coding (STBC) [2, 3]. However, reference [4] shows that even with feedback from the decoder subsequent to the STBC decoder, the performance of the STBC decoder itself will not be improved by soft decoding since there is no new independent extrinsic information. Consequently it is necessary to concatenate an outer channel code with the STBC code in order to enhance the error correcting capability of the system. The turbo code appears to be a good candidate for that purpose. Currently, most of the work on turbo codes has essentially been focused on convolutional turbo codes (CTC), while much less effort has been spent on block turbo codes (BTC).

The system performance comparisons within three different channel codes, that is, convolutional codes, CTC, and BTC, have been studied in [5], which suggests that CTC may be the best choice. Subsequently, another report [6] shows that an iterative maximum a posteriori (MAP) expectation-maximization (EM) algorithm for an STBC-OFDM system in a dispersive channel with a CTC can enable a receiver without channel state information (CSI) to achieve a performance comparable to that of a receiver with perfect CSI.

Yet, some results given in [5] show that BTC outperforms CTC for code rates of $R = 3/4$ and $5/6$. On the other hand, the discussion in [6] points out that such BTC codes have instituted the trellis structure, which can lead to a high complexity because the number of states in the trellis of a block code increases exponentially with the number of redundant bits. Hence those BTC codes may not be practical. Instead, a new BTC is proposed with a balanced compromise between performance and complexity [6]. The proposed BTC can guarantee a minimum distance of 9, while the minimum distance of a CTC can be as low as 2 [7]. If one more check bit is padded to each elementary block code, the minimum distance is increased to 16 for the BTC at the cost of a slightly lower code rate. Another attractive feature of this BTC is that the decoding speed can be increased by employing a bank of parallel elementary decoders for the rows and columns of the product code since they are independent but with the same structure. Hence, we propose here to investigate by means of simulations the receiver performance of an STBC-OFDM system in a dispersive fading channel where

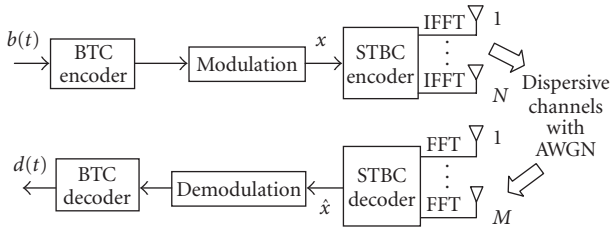

Figure 1: Block diagram of the BTC-STBC-OFDM wireless communication system.

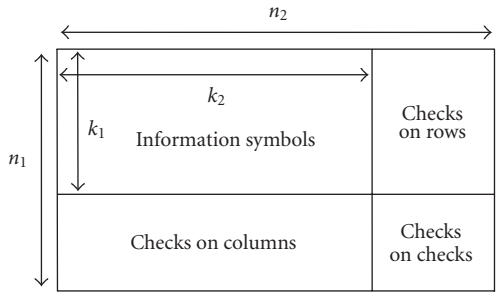

Figure 2: The encoding scheme of the block turbo code.

the BTC is employed as the outer channel code. The simulations are based on four kinds of dispersive channels: two-ray (2R) model, rural area (RA) model, typical urban (TU) model, and hilly terrain (HT) model.

The rest of the paper is organized as follows. Section 2 describes the system model. The soft detection method for the BTC codes is given in Section 3. Section 4 presents the simulation results of the proposed system. Finally, conclusions are drawn in Section 5.

2. SYSTEM MODEL

The system model in a dispersive channel is shown in Figure 1, where AWGN is the additive white Gaussian noise in the channel, $b(t)$ is the information bit stream fed into the BTC encoder, and $d(t)$, an estimate of $b(t)$, is the final recovered bit stream output from the BTC decoder.

An example of a two-dimensional BTC encoding scheme with a code structure of $(n_1, k_1, \delta_1) \times (n_2, k_2, \delta_2)$ is shown in Figure 2, where n_i, k_i, and δ_i $(i = 1, 2)$ denote the length of a codeword, the length of information bits, and the minimum Hamming distance, respectively [6]. The data rate of this BTC encoder is $(k_1 \times k_2)/(n_1 \times n_2)$ and its minimum Hamming distance is $\delta = \delta_1 \times \delta_2$. Such a BTC code can correct up to $s = \lfloor (\delta - 1)/2 \rfloor$ error bits, where $\lfloor X \rfloor$ is the largest integer not greater than the real number X. Thus, a long block code with a large Hamming distance can be constructed by combining short codes with small Hamming distances. The resulting error correction capability will be strengthened significantly.

Subsequent to the BTC encoder, the information stream is modulated by PSK or M-QAM constellations where $M = 16$ or 64. It is then fed to the STBC encoder, where it is processed into N streams according to the STBC encoder design and finally transmitted from N transmit antennas. The details of those modulation schemes can be found in [8, 9]. The data streams are further grouped into K subcarriers after the IFFT and such K subcarriers are independent of one another. The symbols in different subcarriers can be transmitted on the same antenna without introducing additional interference. The diversity gain is N times of that with only one transmit antenna if the appropriate rank criterion [10] has been satisfied.

By adopting Alamouti's scheme [2] in our simulations, the matrix of an encoder with $N = 2$ transmit antennas using the OFDM modulation scheme is

$$G_2 = \begin{bmatrix} \mathbf{x}_1 & \mathbf{x}_2 \\ -\mathbf{x}_2^* & \mathbf{x}_1^* \end{bmatrix} = \begin{bmatrix} \mathbf{c}_{1,1} & \mathbf{c}_{2,1} \\ \mathbf{c}_{1,2} & \mathbf{c}_{2,2} \end{bmatrix}, \tag{1}$$

where $\mathbf{x}_{k_0} = [x_{k_0,0}, x_{k_0,1}, \ldots, x_{k_0,K-1}]^T$ $(k_0 = 1, 2, \ldots, K_0)$ and $x_{k_0,k}$ $(k = 0, 1, \ldots, K-1)$ is the symbol to be transmitted in the kth subcarrier of an STBC-OFDM block composed of K subcarriers, and $\mathbf{c}_{i,t} = [c_{i,t}^0, c_{i,t}^1, \ldots, c_{i,t}^{K-1}]^T$ $(i = 1, 2, \ldots, N$ and $t = 1, 2, \ldots, P)$. Note that both K_0 and P are equal to 2 in the G_2 STBC design and P is the number of OFDM slots, where each OFDM slot contains K symbols. The symbols $c_{i,t}^k$ in the ith column are transmitted by the ith transmit antenna.

For the kth subcarrier, the code is as follows:

$$G_2^k = \begin{bmatrix} x_{1,k} & x_{2,k} \\ -x_{2,k}^* & x_{1,k}^* \end{bmatrix} = \begin{bmatrix} c_{1,1}^k & c_{2,1}^k \\ c_{1,2}^k & c_{2,2}^k \end{bmatrix}, \tag{2}$$

where the superscript "$*$" denotes the conjugation operation. Each OFDM symbol is transmitted after the K-point IFFT.

In the receiver, the signal detected by the jth $(j = 1, 2, \ldots, M)$ antenna after the K-point FFT is

$$\mathbf{r}_{j,t} = \sum_{i=1}^{N} \operatorname{diag}(\mathbf{c}_{i,t}) \mathbf{H}_{i,j} + \eta_{j,t}, \tag{3}$$

where $\mathbf{r}_{j,t} = [r_{j,t}^0, r_{j,t}^1, \ldots, r_{j,t}^{K-1}]^T$ and $\operatorname{diag}(\mathbf{c}_{i,t})$ is a square matrix of order K and its diagonal elements are the elements of the vector $\mathbf{c}_{i,t} = [c_{i,t}^0, c_{i,t}^1, \ldots, c_{i,t}^{K-1}]^T$ and all off-diagonal elements are zero. $\mathbf{H}_{i,j}$ is the channel gain matrix with $\mathbf{H}_{i,j} = [h_{i,j}^0, h_{i,j}^1, \ldots, h_{i,j}^{K-1}]^T$ and $\eta_{j,t}$ is the additive Gaussian noise. For the kth subcarrier, the received signal is

$$r_{j,t}^k = \sum_{i=1}^{N} G_2^k h_{i,j}^k + \eta_{j,t}^k. \tag{4}$$

In dispersive channels, the time-domain channel impulse response $h_{i,j}^k$ can be modeled as a tapped delay line given by

$$h_{i,j}^k = \sum_{l=1}^{L} \alpha_{i,j}^l \exp\left(-\frac{J 2\pi k l}{K} \right), \tag{5}$$

where L is the number of delay taps, J is the unity imaginary number, $\alpha_{i,j}^l$ is the path gain between the ith transmit antenna and the jth receive antenna at the lth delay tap and its value follows the Rayleigh distribution.

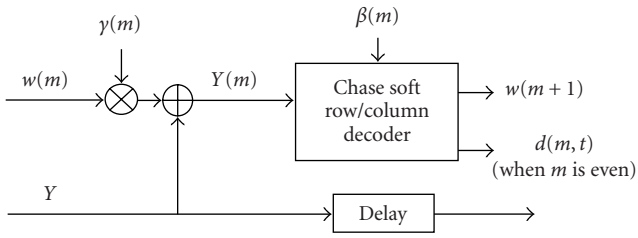

Figure 3: A half-iteration for the BTC soft detection.

In general, the CSI is unknown to the receiver, but it can be assumed to be constant during an STBC-OFDM frame comprising one training STBC block and subsequent STBC data blocks for each subcarrier. In such a case, the estimation can be simplified by calculating (4) and using only the overall $h_{i,j}^k$ instead of the many $\alpha_{i,j}^l$ values in all the taps. Here, the general method of estimating the CSI is adopted [11]. From two long training symbols Tr_1 and Tr_2 that are denoted as G_{Tr} and encoded identically to the design form in (1) [2], covering all K subcarriers, the received signals calculated according to (4) give the channel estimation for each subcarrier as

$$\hat{h}_{i,j}^k = G_{\mathrm{Tr}}^{k^H} \left[r_{j,1_{\mathrm{Tr}}}^k \quad r_{j,2_{\mathrm{Tr}}}^k \right]^T, \tag{6}$$

where the superscript "H" is the Hermite operation. This estimation method is easy to implement without any matrix inversion. If more accurate estimation methods are chosen, the overall performance can be improved further. Without incurring ambiguity, the symbol "$\hat{}$" over h will be omitted in the following description.

After the CSI has been estimated and the received symbols have been successfully separated amongst the different subcarriers, hard decisions for the symbols of the kth subcarrier will be obtained by finding the minimal Euclidean distance from the received codewords [3]:

$$\hat{x}_{1,k} = \underset{x_{1,k}\in\Omega}{\operatorname{argmin}} \left\{ \left| \left[\sum_{j=1}^{M} \left(r_{j,1}^k h_{1,j}^{k*} + r_{j,2}^{k*} h_{2,j}^k \right) \right] - x_{1,k} \right|^2 + \left(\sum_{j=1}^{M} \sum_{i=1}^{2} |h_{i,j}^k|^2 - 1 \right) |x_{1,k}|^2 \right\}, \tag{7}$$

$$\hat{x}_{2,k} = \underset{x_{2,k}\in\Omega}{\operatorname{argmin}} \left\{ \left| \left[\sum_{j=1}^{M} \left(r_{j,1}^k h_{2,j}^{k*} - r_{j,2}^{k*} h_{1,j}^k \right) \right] - x_{2,k} \right|^2 + \left(\sum_{j=1}^{M} \sum_{i=1}^{2} |h_{i,j}^k|^2 - 1 \right) |x_{2,k}|^2 \right\}, \tag{8}$$

where Ω is the symbol constellation of the chosen modulation scheme.

The output of the STBC decoder is then demodulated and decoded by the soft BTC detection to be described in the next section.

3. BTC SOFT DECODER

A BTC soft decoder applies the Chase algorithm [12] iteratively on the rows and columns of a product code. Its main idea is to form test patterns by perturbing the p least reliable bit positions in the received noisy sequence, where p is selected such that $p \ll k$ to reduce the number of reviewed codewords. After decoding the test patterns, the most probable pattern amongst the generated candidate codewords is selected from the codeword D ($D = d_0, \ldots, d_{q-1}$, $q = n_1$ or n_2) which has the minimum Euclidean distance from the received signal Y ($Y = y_0, \ldots, y_{q-1}$). If C ($C = c_0, \ldots, c_{q-1}$) is the most likely competing codeword amongst the candidate codewords with $c_j \neq d_j$, then the reliability information at bit position j is expressed as

$$y_j' = \frac{|Y - C|^2 - |Y - D|^2}{4} d_j, \tag{9}$$

where $|A - B|^2$ denotes the squared Euclidean distance between vectors A and B. The extrinsic information w_j at the jth bit position is found by

$$w_j = \begin{cases} y_j' - y_j & \text{if } C \text{ exists,} \\ \beta d_j & \text{if } C \text{ does not exist,} \end{cases} \tag{10}$$

where β ($\beta > 0$) is a reliability factor to estimate w_j in case no competing codeword C can be found in the test patterns. It is determined empirically. Once the extrinsic information has been determined, the input to the next decoding stage is updated as

$$Y(m) = Y + \gamma(m) w(m), \tag{11}$$

where $\gamma(m)$ is a weighting factor from zero to one and m is the step of the present half-iteration. A half-iteration for a row or column decoding is shown in Figure 3. When m is even, there will be a hard decision output $d(m, t)$. The procedures described above are then iterated for the remaining column (or row) decoding.

In [13], the complexities of different kinds of channel decoders have been investigated. For a CTC$(2, 1, \xi)$, the complexity per bit is approximated as

$$\begin{aligned} \mathrm{comp}\{\mathrm{CTC}(2,1,\xi)\} &= 3 \times 2 \times 2^{\xi-1} \times 2 \times \text{ no. of iterations} \\ &= 3 \times 2^{\xi+1} \times \text{ no. of iterations.} \end{aligned} \tag{12}$$

For a BTC$(n, k) \times (n, k)$, the corresponding complexity per bit is approximated as

$$\begin{aligned} &\mathrm{comp}\{\mathrm{BTC}(n,k) \times (n,k)\} \\ &\quad = 3 \times 2 \times \left[(2k - n + 2) \times \frac{2^{n-k}}{k} \right] \times 2 \times \text{ no. of iterations} \\ &\quad = 3 \times (2k - n + 2) \times 2^{n-k+2} \times \frac{\text{no. of iterations}}{k}. \end{aligned} \tag{13}$$

Since the operations in (9), (10), and (11) can be implemented in parallel, the detection efficiency of a BTC can be further improved at least k times, which makes BTC decoding even faster.

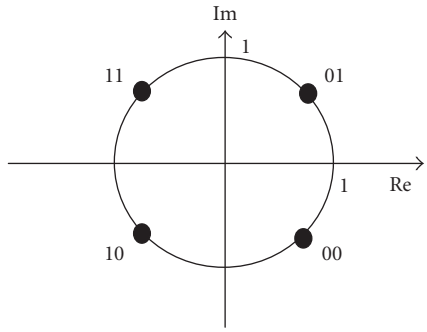

Figure 4: Gray mapping for $\pi/4$ QPSK modulation.

When the above soft detection is included in the proposed system, some modifications to (7) and (8) are needed. Taking BPSK modulation as an example, (7) should be changed to

$$\hat{x}_{1,k} = \text{sign}\left(\text{real}\left(\sum_{j=1}^{M}\left(r_{j,1}^{k}h_{1,j}^{k*} + r_{j,2}^{k*}h_{2,j}^{k}\right)\right)\right). \tag{14}$$

Therefore, the initial reliability value for $\hat{x}_{1,k}$ is

$$y_{1,k} = \text{real}\left(\sum_{j=1}^{M}\left(r_{j,1}^{k}h_{1,j}^{k*} + r_{j,2}^{k*}h_{2,j}^{k}\right)\right). \tag{15}$$

Similarly, the initial reliability value for $\hat{x}_{2,k}$ is

$$y_{2,k} = \text{real}\left(\sum_{j=1}^{M}\left(r_{j,1}^{k}h_{2,j}^{k*} - r_{j,2}^{k*}h_{1,j}^{k}\right)\right). \tag{16}$$

For QPSK modulation, two bits comprise a symbol and the frequently used $\pi/4$ Gray mapping scheme shown in Figure 4 is adopted. Then according to the mapping and (7), the initial reliability values for each bit in $\hat{x}_{1,k}$ can be represented as

$$\begin{aligned} y_{1,k}^{1} &= \text{real}\left(\sum_{j=1}^{M}\left(r_{j,1}^{k}h_{1,j}^{k*} + r_{j,2}^{k*}h_{2,j}^{k}\right)\right), \\ y_{1,k}^{2} &= \text{imag}\left(\sum_{j=1}^{M}\left(r_{j,1}^{k}h_{1,j}^{k*} + r_{j,2}^{k*}h_{2,j}^{k}\right)\right). \end{aligned} \tag{17}$$

Similarly, the initial reliability values for each bit in $\hat{x}_{2,k}$ can be represented as

$$\begin{aligned} y_{2,k}^{1} &= \text{real}\left(\sum_{j=1}^{M}\left(r_{j,1}^{k}h_{2,j}^{k*} - r_{j,2}^{k*}h_{1,j}^{k}\right)\right), \\ y_{2,k}^{2} &= \text{imag}\left(\sum_{j=1}^{M}\left(r_{j,1}^{k}h_{2,j}^{k*} - r_{j,2}^{k*}h_{1,j}^{k}\right)\right). \end{aligned} \tag{18}$$

For the QAM-16 or QAM-64 scheme [8, 9], the reliability values for each bit in a symbol are calculated by separating the received symbols in several levels as described in [8].

When all the initial reliability values for a BTC codeword have been obtained, soft detection can be performed with the iterative Chase algorithms.

4. SIMULATIONS

The binary BCH (15,11,3)-code is used in both the row and column encoding in our simulations. Thus, the data rate is 121/225, the Hamming distance is $\delta = 9$, and the error correction capability is $s = 4$. The QPSK modulation and the G_2 STBC coding given in (1) are employed with two receive antennas ($M = 2$) and $K = 128$ subcarriers. To obtain a better error correcting capability with a slightly lower transmission rate, one check bit is actually padded to each row or column code, that is, the BCH (16,11,4)-code is applied with a code rate of 121/256 and a Hamming distance of 16 with an error correction capability $s = 7$. The resulting BTC $(16, 11, 4) \times (16, 11, 4)$-code comprises two OFDM blocks and hence one STBC-OFDM block. According to (13), the complexity is about 279 for each iteration step. If parallel decoding is implemented with more memory, the averaged complexity per bit is approximated as $279/11 \approx 25$. On the other hand, the convolutional code (2,1,3) adopted in the CTC scheme [11] has a corresponding complexity of 96 per bit for each iteration step according to (12), which is obviously larger than 25. Therefore, the proposed system using BTC should be more efficient than the one using CTC.

To make a fair comparison with results using CTC as the outer channel code [11], similar modeling parameters are adopted in the present simulations. The available bandwidth is 800 kHz and is divided into 128 subcarriers. The symbol rate in each subcarrier is 5000 symbols/s ($T_s = 1/5000 = 0.0002$ second) and one OFDM data word lasts 160 microseconds. In each OFDM word, a cyclic prefix interval of 40 microseconds is added to combat the effect of interblock interference. Hence, the duration of one complete OFDM word is 200 microseconds. Therefore, the total information rate is reduced to 0.7563, which is comparable with the rate 0.8 in [11]. The OFDM system transmits in data bursts, each consisting of 22 OFDM words. The first two OFDM words are the training symbols and the next 20 OFDM words span over the duration of 10 STBC codewords. Simulation results are shown in terms of the bit error rate (BER) performance versus the signal-to-noise ratio (SNR). The soft detection parameters are $\gamma = [0\ \ 0.2\ \ 0.3\ \ 0.5\ \ 0.7\ \ 0.9\ \ 1\ \ 1\ \ 1\ \ 1]$, $\beta = [0.2\ \ 0.4\ \ 0.6\ \ 0.8\ \ 1\ \ 1\ \ 1\ \ 1\ \ 1\ \ 1]$, $p = 4$ and five iterations are performed.

The receiver performance is simulated with different delay profiles in four typical channel models described in COST 207 [14], namely the two-ray (2R) model, the typical urban (TU) model, the hilly terrain (HT) model, and the rural area (RA) model with a Doppler frequency of $f_d = 50$ Hz ($f_d T_s = 0.01$) or $f_d = 200$ Hz ($f_d T_s = 0.04$). The latter three channels have six different paths. The corresponding channel profiles, that is, the delays and fading gains of the paths, are shown in Table 1 [14].

The simulation results of our proposed BTC algorithm for the four channel models are shown in Figure 5 for

Table 1: Channel parameters: delay (μs)/fading gain. The path fading gain with # is equal to 0 dB.

Model	Path 1	Path 2	Path 3	Path 4	Path 5	Path 6
2R	0.0/1.000#	0.1/0.500	—	—	—	—
TU	0.0/0.189	0.2/0.379#	0.5/0.239	1.6/0.095	2.3/0.061	5.0/0.037
HT	0.0/0.413#	0.1/0.293	0.3/0.145	0.5/0.074	15.0/0.066	17.2/0.008
RA	0.0/0.602#	0.1/0.241	0.2/0.096	0.3/0.036	0.4/0.018	0.5/0.006

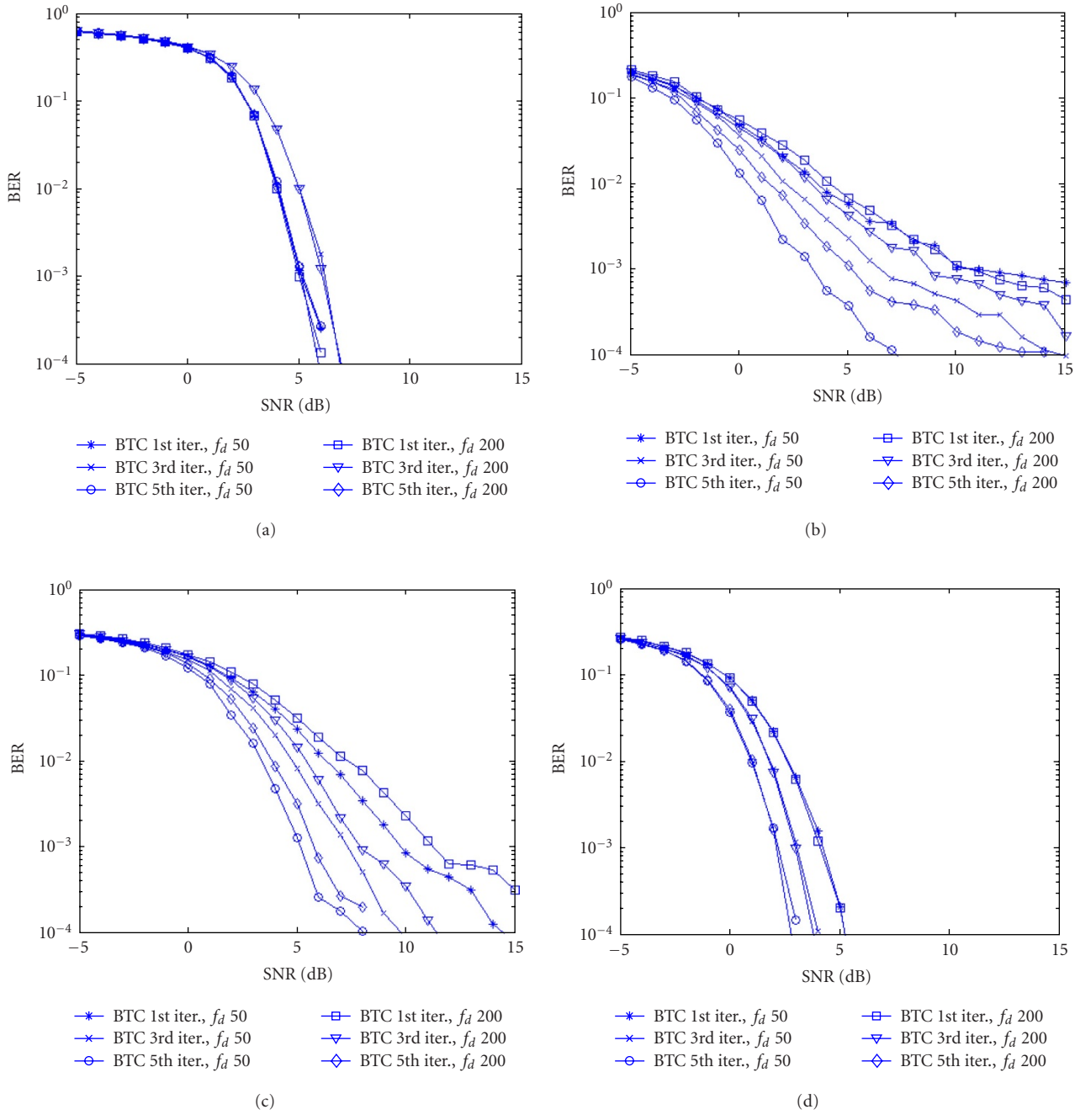

Figure 5: The BER performance for the BTC-based STBC-OFDM system in different dispersive channels with the Doppler frequency equal to 50 Hz and 200 Hz, respectively: (a) 2R: two ray; (b) TU: typical urban; (c) HT: hilly terrain; (d) RA: rural area.

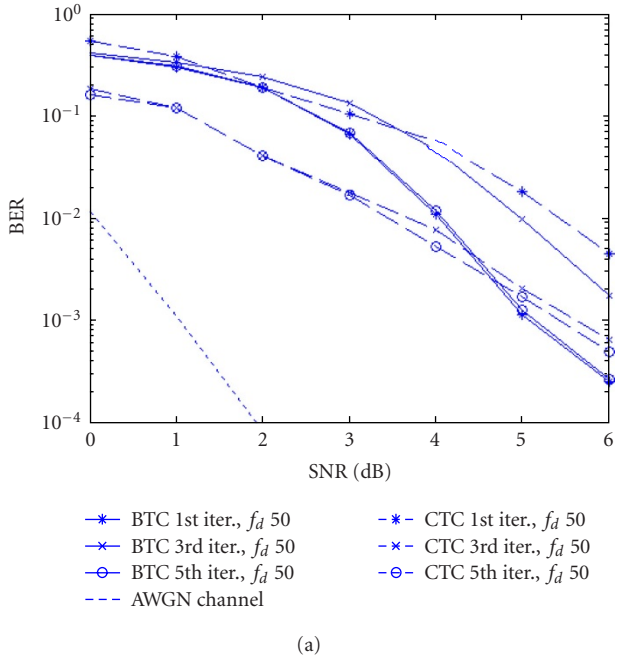

(a)

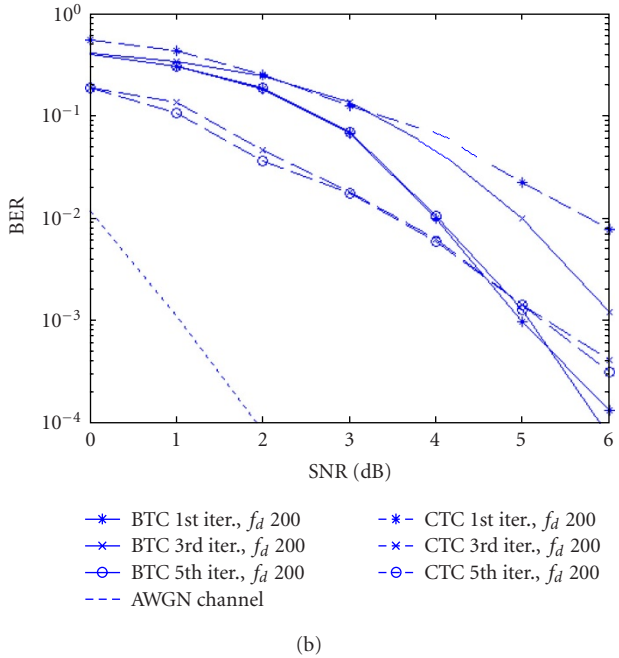

(b)

Figure 6: The BER performance comparison with different Doppler frequencies in 2R channels: (a) 50 Hz; (b) 200 Hz.

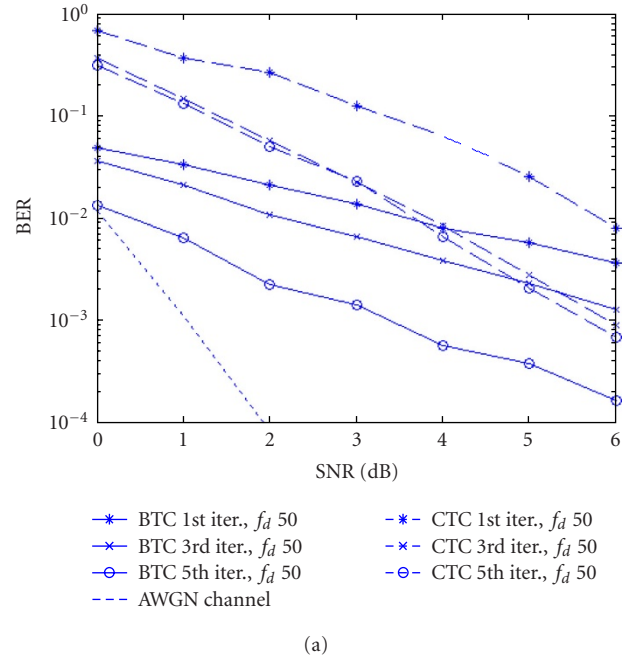

(a)

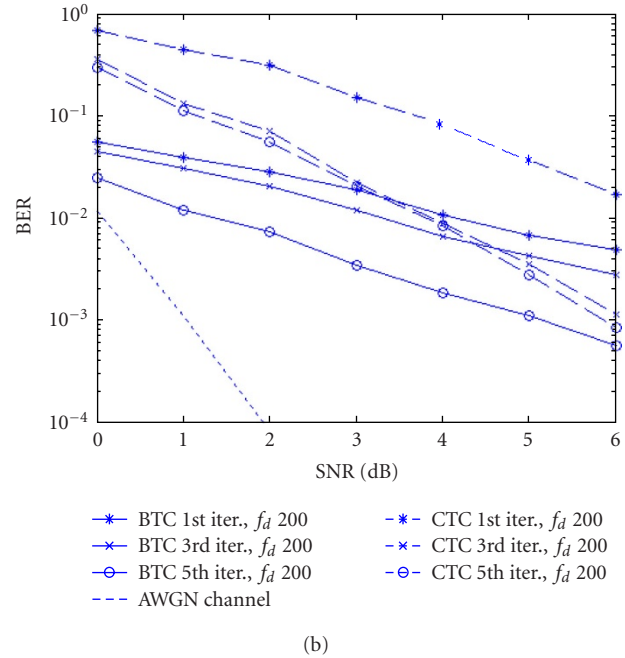

(b)

Figure 7: The BER performance comparison with different Doppler frequencies in TU channels: (a) 50 Hz; (b) 200 Hz.

different Doppler frequencies. For all the models, iteration gain has been obtained. For the 2R model, the iteration gain appears only between the first and the third iterations but the fifth iteration shows little gain over the third iteration. In the latter three models, it can be predicted that the BER performance can be further improved with more iterations. Not surprisingly, the performance in the RA model surpasses those in the other three models since the RA model is similar to the ideal free-space model.

The results for the iterative turbo receiver with MAP-EM algorithm in the STBC-OFDM system are given for different models and different Doppler frequencies in Figures 6, 7, 8 and 9 where the performance of the concatenated STBC-BTC system in an AWGN channel after four iterations [15] is also shown as a reference. The comparison shows that the proposed BTC-based system outperforms the CTC-based system in almost any environment, except where the SNR is from 0 dB to 4.5 dB in the 2R model. The SNR improvements at

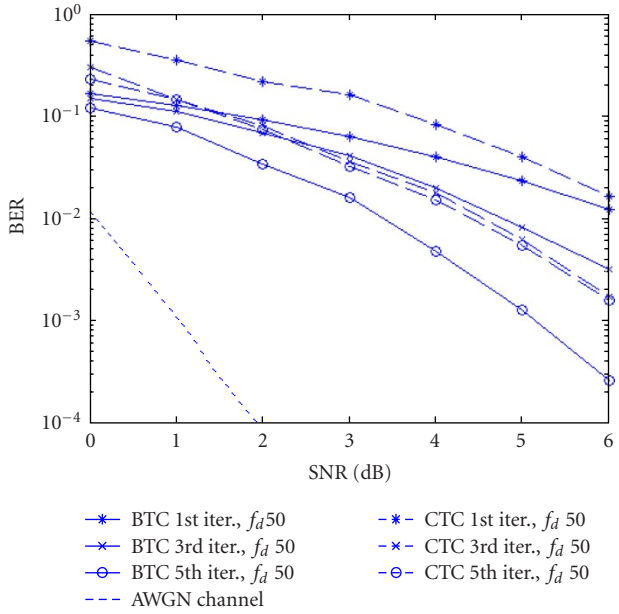

(a)

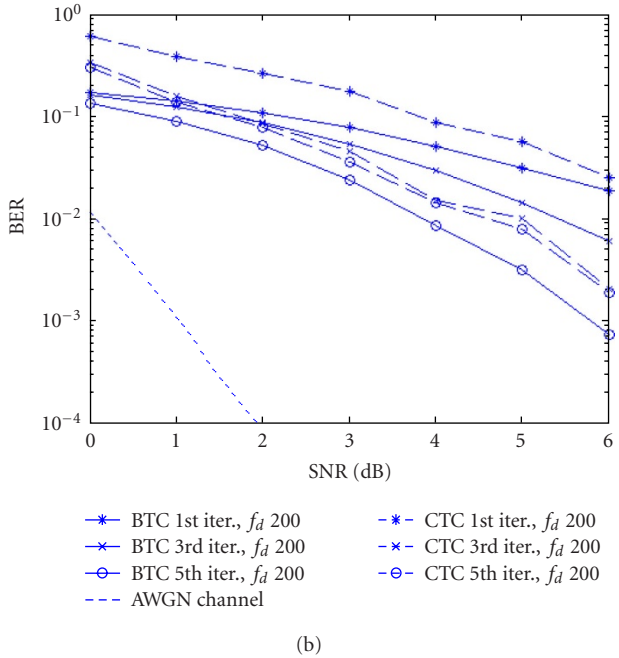

(b)

Figure 8: The BER performance comparison with different Doppler frequencies in HT channels: (a) 50 Hz; (b) 200 Hz.

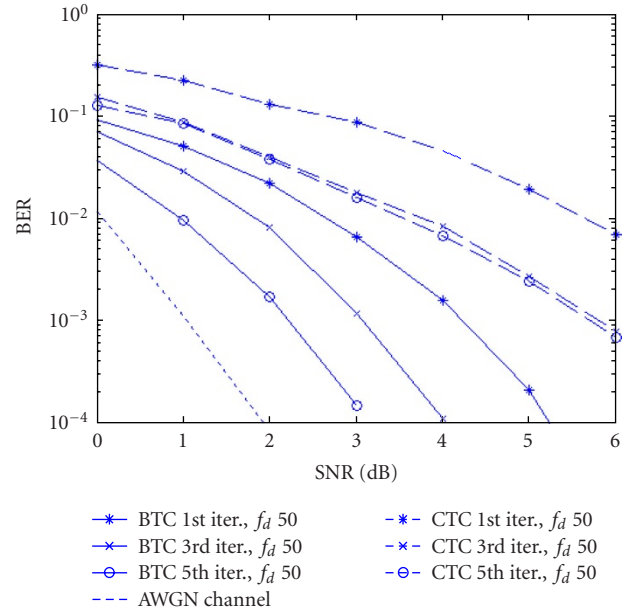

(a)

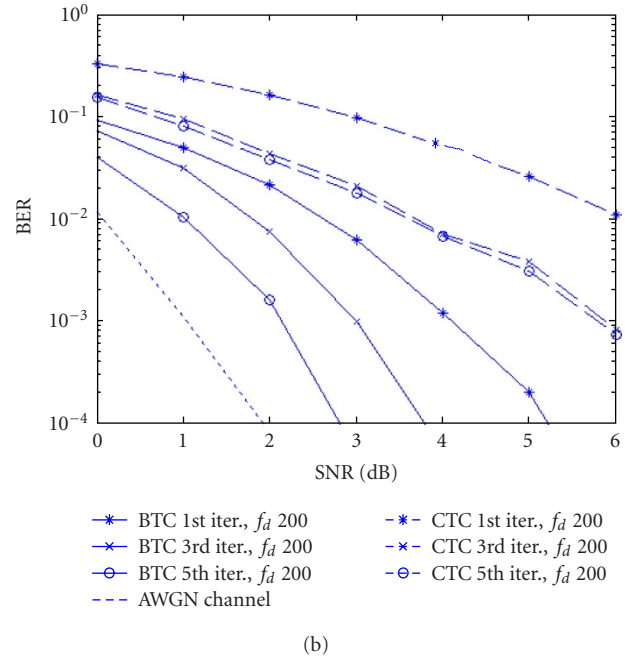

(b)

Figure 9: The BER performance comparison with different Doppler frequencies in RA channels: (a) 50 Hz; (b) 200 Hz.

the fifth iteration and at the BER value of 10^{-3} for all the cases considered are shown in Table 2. Clearly, there is an improvement of about 0.2 $\sim$ 3.6 dB. All these results confirm the validity and advantage of the BTC-based STBC-OFDM system in dispersive channels. However, in the TU model (Figures 5b and 7) and HT model (Figure 5c), the proposed systems also exhibit asymptotic error floors at high SNR values, which shows the sensitivity of OFDM in the presence of large Doppler shifts. Then, a single-carrier transmission system [16, 17] employing the Alamouti scheme on a block basis rather than the symbol basis may be a better choice than OFDM. Here, the OFDM technique is adopted just for a fair comparison as it is also used in the STBC-OFDM-CTC system [11].

5. CONCLUSIONS

The performance of a BTC-based STBC-OFDM system in dispersive channels has been investigated in this paper. The good error correcting capability of BTC and the large

Table 2: SNR improvement of BTC-STBC-OFDM over CTC-STBC-OFDM at the fifth iteration and at the BER of 10^{-3}.

Doppler frequency (Hz)	SNR improvement (dB)			
	2R model	TU model	HT model	RA model
50	0.3	2.3	1.2	3.5
200	0.2	0.7	0.7	3.6

diversity gain characteristics of STBC can be achieved simultaneously. The simple concatenation of STBC and BTC leads to a better BER performance than that of the CTC-based STBC-OFDM system using the iterative turbo receiver with the MAP-EM algorithm in any kind of simulated dispersive fading channels. Furthermore, since the row (or column) encoding (or decoding) of the BTC coding can be implemented in parallel, the computation efficiency can be further improved. The simulation results confirm the validity of the proposed system.

REFERENCES

[1] R. van Nee and R. Prasad, *OFDM for Wireless Multimedia Communications*, Artech House Publishers, Boston, Mass, USA, 2000.

[2] S. M. Alamouti, "A simple transmit diversity technique for wireless communications," *IEEE J. Select. Areas Commun.*, vol. 16, no. 8, pp. 1451–1458, 1998.

[3] V. Tarokh, H. Jafarkhani, and A. R. Calderbank, "Space-time block coding for wireless communications: performance results," *IEEE J. Select. Areas Commun.*, vol. 17, no. 3, pp. 451–460, 1999.

[4] G. Bauch, "Concatenation of space-time block codes and "turbo"-TCM," in *Proc. IEEE International Conference on Communications (ICC' 99)*, vol. 2, pp. 1202–1206, Vancouver, British Columbia, Canada, June 1999.

[5] B. L. Yeap, T. H. Liew, J. Hamorsky, and L. Hanzo, "Comparative study of turbo equalization schemes using convolutional, convolutional turbo, and block-turbo codes," *IEEE Trans. Wireless Communications*, vol. 1, no. 2, pp. 266–273, 2002.

[6] R. M. Pyndiah, "Near-optimum decoding of product codes: block turbo codes," *IEEE Trans. Commun.*, vol. 46, no. 8, pp. 1003–1010, 1998.

[7] R. Garello, F. Chiaraluce, P. Pierleoni, M. Scaloni, and S. Benedetto, "On error floor and free distance of turbo codes," in *Proc. IEEE International Conference on Communications (ICC' 01)*, vol. 1, pp. 45–49, Helsinki, Finland, June 2001.

[8] R. Pyndiah, A. Picart, and A. Glavieux, "Performance of block turbo coded 16-QAM and 64-QAM modulations," in *Proc. IEEE Global Telecommunications Conference (GLOBECOM '95)*, vol. 2, pp. 1039–1043, Singapore, November 1995.

[9] ETSI EN 300 744 V1.4.1, " http://www.ttv.com.tw/TVaas/file/En300744.V1.4.1.pdf," .

[10] V. Tarokh, N. Seshadri, and A. R. Calderbank, "Space-time codes for high data rate wireless communication: performance criterion and code construction," *IEEE Trans. Inform. Theory*, vol. 44, no. 2, pp. 744–765, 1998.

[11] B. Lu, X. Wang, and Y. Li, "Iterative receivers for space-time block-coded OFDM systems in dispersive fading channels," *IEEE Trans. Wireless Communications*, vol. 1, no. 2, pp. 213–225, 2002.

[12] D. Chase, "Class of algorithms for decoding block codes with channel measurement information," *IEEE Trans. Inform. Theory*, vol. 18, no. 1, pp. 170–182, 1972.

[13] T. H. Liew and L. Hanzo, "Space-time codes and concatenated channel codes for wireless communications," *Proc. IEEE*, vol. 90, no. 2, pp. 187–219, 2002.

[14] G. L. Stüber, *Principles of Mobile Communication*, Kluwer Academic Publishers, Boston, Mass, USA, 2001.

[15] Y. Du and K. T. Chan, "Enhanced space-time block coded systems by concatenating turbo product codes," *IEEE Commun. Lett.*, vol. 8, no. 6, pp. 388–390, 2004.

[16] N. Al-Dhahir, "Single-carrier frequency-domain equalization for space-time block-coded transmissions over frequency-selective fading channels," *IEEE Commun. Lett.*, vol. 5, no. 7, pp. 304–306, 2001.

[17] E. Lindskog and A. Paulraj, "A transmit diversity scheme for channels with intersymbol interference," in *Proc. IEEE International Conference on Communications (ICC' 00)*, pp. 307–311, New Orleans, La, USA, June 2000.

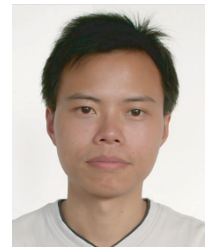

Yinggang Du received his Bachelor of Engineering and Master of Engineering degrees in 1997 and 2000, respectively, both from the Department of Electronic Engineering, Nanjing University of Science & Technology (NJUST). He obtained the Ph.D. degree in October 2004 from the Department of Electronic Engineering, The Chinese University of Hong Kong (CUHK). He acted as an Assistant Professor from April 2000 at NJUST and a Teaching Assistant from October 2000 to September 2003 in CUHK. He has been a research assistant since October 2003 in CUHK. He is an IEEE Member now and his present research interests include space-time coding, radar signal processing, wireless communications, genetic algorithm, and digital signal processing.

Kam Tai Chan received his Ph.D. degree from Cornell University in applied physics in March 1986. His thesis research involved the preparation of ultrathin compound semiconductor materials for optoelectronics and quantum-size effect devices. He stayed at Cornell University as a Postdoctoral Research Associate to work on high-power lasers and integrated photodetectors after graduation. He joined Microwave Technology Division, Hewlett-Packard Company in July 1986. He participated in projects that were related to photodetectors and high electron mobility transistors. In 1989 he was invited by Lawrence Berkeley Laboratory of the Berkeley University of California to serve as a Visiting Industrial Fellow to develop industrial applications of the extensive sophisticated instrumentation in the laboratory. He resigned from Hewlett-Packard at the end of 1991 to assume his present position at the Chinese University of Hong Kong. He is a Member of IEEE and his present research interests include ultrafast lasers, novel photonic devices, optical switches, optical CDMA, wireless communication, and quantum cryptography.